SNRU Journal of Science and Technology

Journal home page: snrujst.snru.ac.th

The comparison behaviors of some scintillators for radiation shielding

Sunantasak Ravangvong[1,*], Kittisak Sriwongsa[2,3], Punsak Glumglomchit[4], Ratchanon Janthimangkul[4], Maysinee Pansuay[4], Salinya Puangfuang[4], Nopparat Suksee[4], Chumphon Khobkham[5]

[1]Division of Science and Technology, Faculty of Science and Technology, Phetchaburi Rajabhat University, Phetchaburi, 76000 Thailand

[2]Faculty of Education, Silpakorn University, Nakhon Pathom, 73000 Thailand

[3]The demonstration school of Silpakorn University, Nakhon Pathom, 73000 Thailand

[4]Huahin Vitthayalai School, Hua–Hin, Prachuap Khiri Khan, 77110 Thailand

[5]Faculty of Engineering, Thonburi University, Bangkok, 10160 Thailand

[*]**Corresponding Author**: sunantasak.rav@mail.pbru.ac.th

Received: 7 May 2021; **Revised:** 12 July 2021; **Accepted:** 26 August 2021; **Available online:** 1 January 2022

Abstract

In this research, the photon interaction of NaI:Tl, LiI:Tl and CsI:Tl scintillators have been comparative studied. The photon interaction effectiveness of scintillators was investigated by determine mass attenuation coefficient (μ_m) and half value layer (*HVL*) at photon energy ranging 1 keV – 100 GeV using WinXCom computer software program. Build–up factors were computed by Geometric Progression (G–P) fitting formula at energy ranging 15 keV – 15 MeV up to 40 mfp penetration depth. The result shown that, CsI:Tl scintillator was excellent at interacting with photons. This study indicated that CsI:Tl can be developed for radiation detectors and sensors.

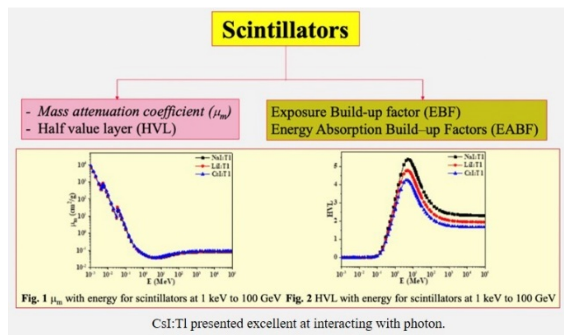

Keywords: Scintillator; Photon interaction; Build–up factors

1. Introduction

Now a day, scintillator materials have been used widely in many sectors of ionizing radiation detection such as technology of medical and astrophysical, high-energy particle in physics, nuclear fusion reactor [1, 2]. To apply and utilizing the scintillator materials, the fundamental knowledge for probability of photon interaction values such as μ_m, half value layer (*HVL*) and build–up factors (BFs) is important value to considered [3, 4]. Due to these values discuss the penetration of ionizing radiation in medium. These values are related to each other which *HVL* and BFs values can be obtained using μ_m value [5]. So, the accurate μ_m is required because of this value is basic result has been used to explained in several ionizing radiation sectors such as clinical computed tomography (CT) [6], gamma densitometry [7] and radiation shielding [8].

In the sector of radiation interaction with medium, the probability of interaction will high when medium had large atomic number and density. Scintillator once of material which has high atomic number and density, in addition there are several researchers were studied the radiation interaction [5, 9, 10]. NaI:Tl scintillator, one of scintillator which easy to prepared, cheap and widely used in neutron and X/γ ray detectors [11, 12] as well as LiI:Tl and CsI:Tl scintillators are widely use under neutron and X/γ ray [13, 14].

In this context, the quantities of photon interaction for scintillators were calculated. The values of photon interaction, μ_m and *HVL* were simulated at energy ranging 1 keV – 100 GeV by WinXCom program which these energy ranging were covered the main photon interaction (photoelectric effect, Compton scattering and pair production) while BFs (exposure build-up and energy absorption build–up factors; EBF and EABF) were computed at energy ranging 15 keV – 15 MeV using G–P fitting.

2. Materials and Methods

Mass attenuation coefficient and half value layer

μ_m of scintillators was calculated theoretically by using mixture rule and WinXCOM software program and using following by Eq. (1) [15, 16]:

$$\mu_m = \sum_{i=1}^{n} w_i \mu_{mi} \quad (1)$$

here w_i and μ_{mi} are weight fraction and mass attenuation coefficients of constituent elements, respectively.

HVL of scintillators was evaluated by using linear attenuation coefficient (μ) as following by Eq. (2) [17, 18]:

$$HVL = \frac{0.693}{\mu} \quad (2)$$

Build–up factors

The *BFs* are basically value used design medium for radiation shielding. BFs separated two types, 1. EBF and 2. EABF which obtained by computing from G–P fitting method at energy ranging 0.015 – 15 MeV and these values can be following Eq. (3 – 5). Firstly, it is very important to know that the equivalent atomic number (Z_{eq}) values must lie at specific energy between Z_1 and Z_2 atomic numbers ($Z_1 < Z_{eq} < Z_2$) [19, 20].

$$B(E,x) = 1 + \frac{b-1}{K-1}(K^x - 1), K \neq 1 \quad (3)$$

$$B(E,x) = 1 + (b-1)\,x, K = 1 \quad (4)$$

where E and K are photon energy and photon dose multiplication factor, respectively and K was obtained from Eq. (5):

$$K(E,x) = cx^a + d\frac{\tanh\left(\frac{x}{x_k} - 2\right) - \tanh(-2)}{1 - \tanh(-2)}, x \leq 40 \text{ mfp} \quad (5)$$

here x is deep penetration in mfp (cm), and b is buildup factor at 1 mfp and a, b, c, d and X_k are G–P fitting parameters.

3. Results and Discussion

The samples and properties for scintillators are listed in Table1. The μ_m and *HVL* with energy for scintillators were presented in Fig. 1 and 2, respectively.

The EBF and EABF values of scintillators with energies were presented in Fig. 3 – 6.

Table 1 Properties of some scintillators.

Sample	Density (g cc^{-1})	Ref.
NaI:Tl	3.67	[21, 22]
LiI:Tl	4.10	[22]
CsI:Tl	4.51	[21]

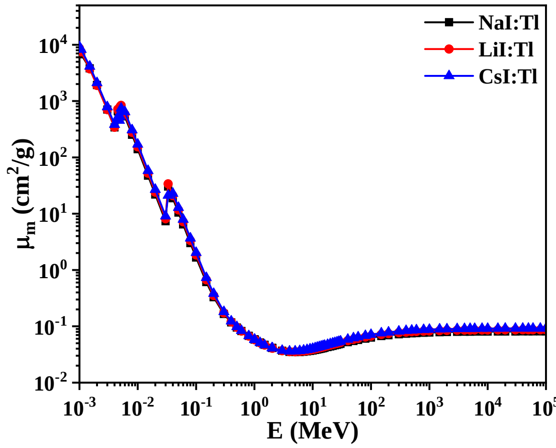

Fig. 1 μ_m with energy for scintillators at 1 keV to 100 GeV.

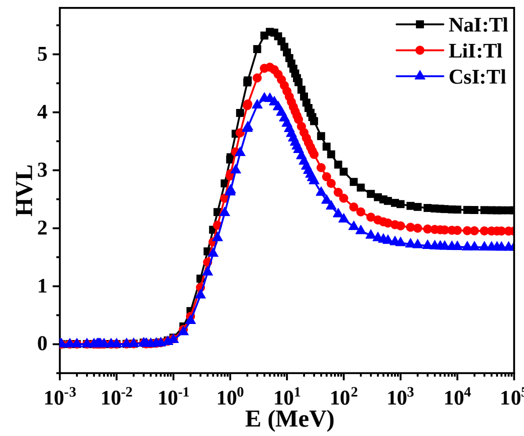

Fig. 2 *HVL* with energy for scintillators at 1 keV to 100 GeV.

Mass Attenuation Coefficient

Photoelectric absorption effect (PE), Compton scattering (C) and pair production (PP) interaction are important processes of photon with medium. These interactions of scintillator can be discussed by total μ_m with photon energy, as shown in Fig. 1. This figure exhibits that at low energy ranging (E < 0.15 MeV), intermediate energy ranging (0.15 < E < 1.50 MeV), and high energy ranging (E > 1.5 MeV) are three energy ranging for interaction processes. From Fig. 1, the μ_m values of scintillators decrease quickly, from 7.801×10^3 to 6.112×10^{-1}, 8.636×10^3 to 6.676×10^{-1} and 9.234×10^3 to 7.291×10^{-1} cm^2 g^{-1} for NaI:Tl, LiI:Tl and CsI:Tl for scintillator, respectively, and energy increases up to 0.15 MeV. At these energy ranging, graphs are not continuous because of K–, L–, and M–absorption edges, as shown in Table 2 due to PE. This μ_m behavior with energy may be PE cross–section which according to $E^{3.50}$. At energy ranging 0.15 < E < 1.50 MeV, μ_m values for scintillators vary slowly, from 0.661 to 0.047, 0.668 to 0.046 and 0.729 to 0.046 cm^2 g^{-1} for NaI:Tl, LiI:Tl and CsI:Tl, respectively. This μ_m values is difference due to process of C is main mechanism. As, C cross–section process is according to E^{-1} and linearly varies with Z number. At energy ranging 1.50 MeV – 100 GeV, μ_m values increase slowly like constant and high. This result indicated that μ_m values were depend on composition of scintillators and PP is main one. Lastly, the results shown that CsI:Tl scintillator had the highest μ_m.

Half value layer

The *HVL* result is the most suitable quantity explaining photon interaction with material. For the best photon interaction with material, lower *HVL* value is required. The *HVL* values as a function of photon energy are plotted in Fig. 2. From figure, at photon energy ranging 1 – 80 keV, *HVL* are independent from the sample composition. And then, *HVL* values increase until energy increases to 5, 5 and 4 MeV for NaI:Tl, LiI:Tl and CsI:Tl, respectively. Above 3 GeV, *HVL* values are depended on composition of scintillators, and *HVL* values of CsI:Tl is lower than NaI:Tl and LiI:Tl. The result of *HVL* indicated that CsI:Tl is excellent photon interaction.

EBF and EABF values with energy ranging 15 keV – 15 MeV at 1, 5, 10, 15, 20, 25, 30, 35 and 40 mfp deep penetration of scintillators mediums have been exhibited in Fig. 3 – 4. These figure presents that the EBF and EABF maximum values are depended on composition of scintillator and deep penetration. It is clearly that EBF and EABF values increase until maximum value with increasing energy, and then decrease with increasing energy. At low energy ranging, EBF and EABF values are lowest due to a great amount photon were absorbed which PP is main interaction process. At intermediate energy ranging, EBF and EABF values are highest due to C is main interaction process. At high energy ranging, photons have been absorbed again due to PP is main interaction process. The results of EBF and EABF for scintillators have sharp magnitude which may be occurred from K–absorption edges for each element. Due to multiple scattering were occurred at high deep penetration so the highest values of EBF and EABF were found at 40 mfp deep penetration while the lowest values were found at 1 mfp. Fig. 5 – 6 present EBF and EABF with deep penetration for scintillators at 1, 10, 20 and 40 mfp. CsI:Tl scintillator had the smallest EBF and EABF values, this indicate that CsI:Tl scintillator is excellent at interacting with photons.

Table 2 Absorption edges (keV) for element.

Element	**Z**	**K**	**L_1**	**L_2**	**L_3**	**M_1**	**M_2**
Na	11	1.072					
I	53	33.170	5.188	4.852	4.557	1.072	
Cs	55	35.980	5.714	5.359	5.012	1.217	1.065

Exposure Buildup Factors and Energy Absorption Buildup Factors

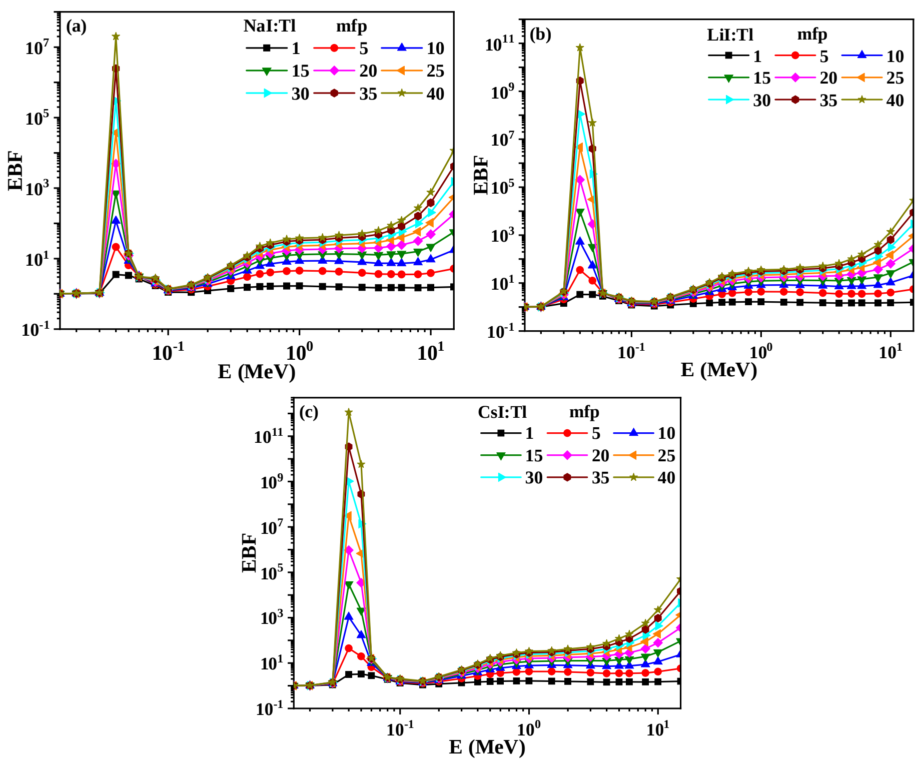

Fig. 3(a – c): EBF for scintillators with energy at 1, 5, 10, 15, 20, 25, 30, 35 and 40 mfp.

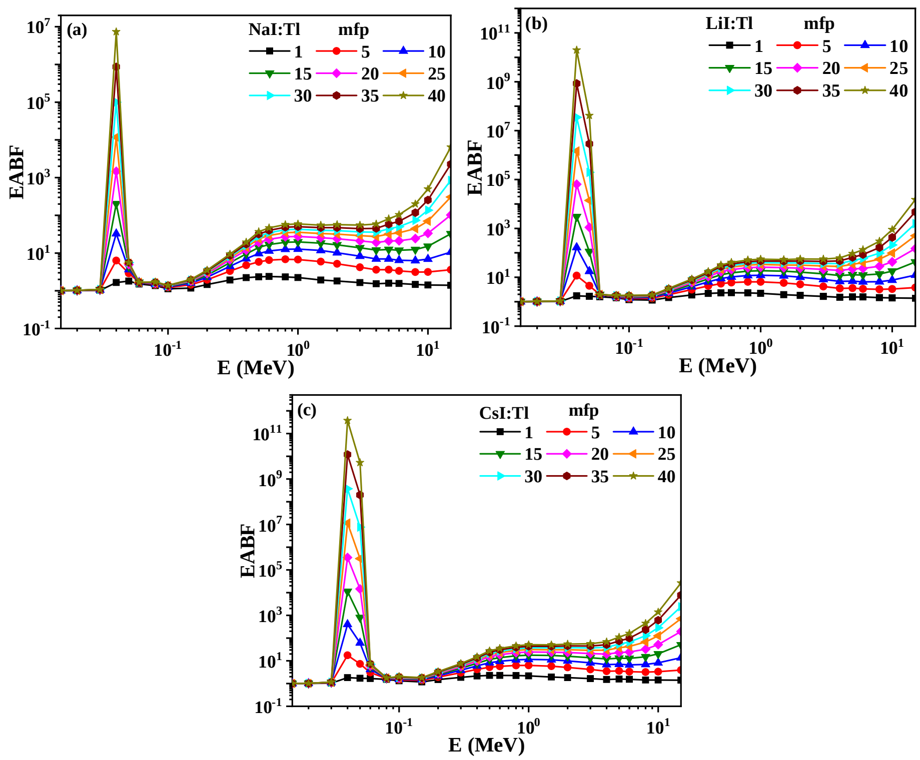

Fig. 4(a – c): EABF for scintillators with energy at 1, 5, 10, 15, 20, 25, 30, 35 and 40 mfp.

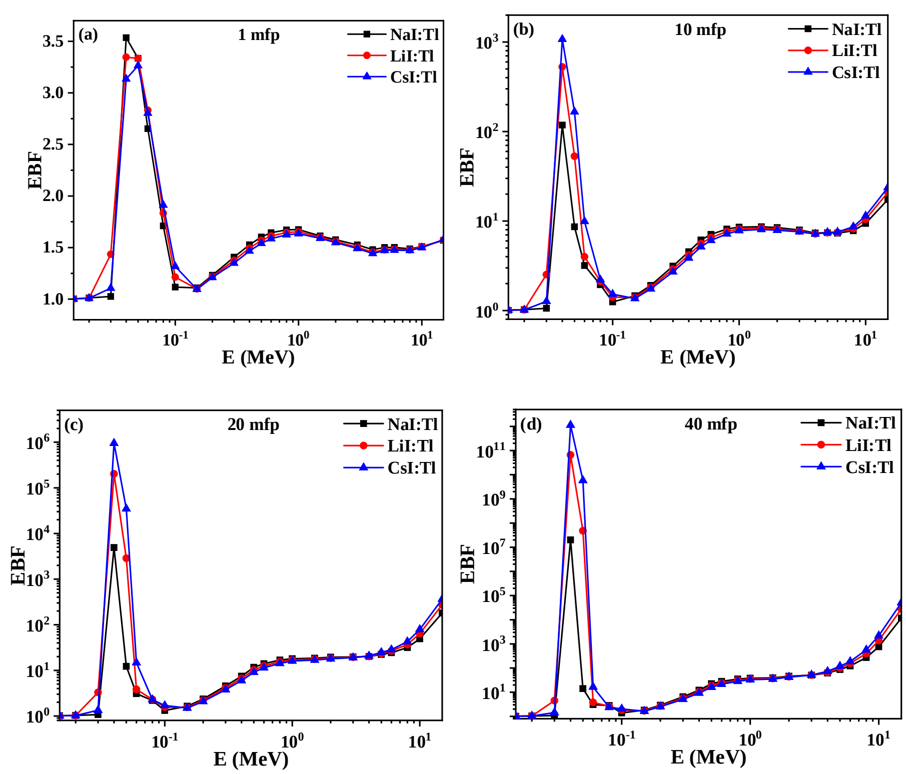

Fig. 5(a – d): EBF with energy at 1, 10, 20 and 40 mfp.

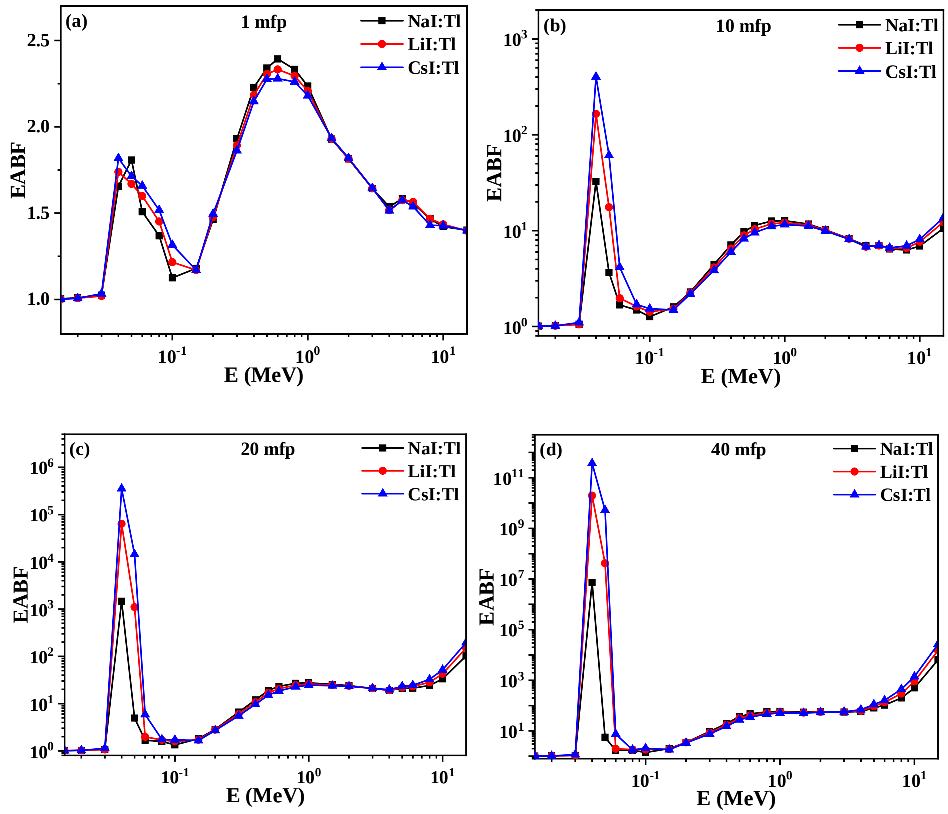

Fig. 6(a – d): EABF with energy at 1, 10, 20 and 40 mfp.

4. Conclusion

The photon interaction with materials values, mass attenuation coefficient and half value layer have been determined using WinXCom software program at energy ranging 1 keV – 100 GeV of NaI:Tl, LiI:Tl and CsI:Tl scintillators. The EBF and EABF values at energy ranging 15 keV – 15 MeV and deep penetration until 40 mfp have been estimated using G–P fitting method for all scintillators.The estimating values indicated that CsI:Tl presented excellent at interacting with photons because of it had the highest mass attenuation coefficient values while half value layer and buildup factors values lowest.

5. Acknowledgement

The authors gratefully acknowledge Phetchaburi Rajabhat University for support the measuring instrument.

6. References

[1] J. Pejchal, J. Barta, T. Trojek, R. Kucerkova, A. Beitlerova, M. Nikl, Luminescence and scintillation properties of rare-earth-doped $LaAlO_3$ single crystals, Radiat. Meas. 121 (2019) 26 – 31.

[2] J. Oliveira, V. Correia, P. Costa, A. Francesko, G. Rocha, S. Lanceros–Mendez, Stretchable scintillator composites for indirect X-ray detectors, Compos. Part B. 133 (2018) 226 – 231.

[3] M.I. Sayyed, Y. Elmahroug, B.O. Elbashir, Shams A.M. Issa, Gamma–ray shielding properties of zinc oxide soda lime silica glasses, J. Mater. Sci: Mater Electron. 28 (2017) 4064 – 4074.

[4] S.A.M. Issa, Y.B. Saddeek, M.I. Sayyed, H.O. Tekin, O. Kilicoglu, Radiation shielding features using MCNPX code and mechanical properties of the $PbO–Na_2O–B_2O_3–CaO–Al_2O_3–SiO_2$ glass systems, Compos. B. 167 (2019) 231 – 240.

[5] S.A.M. Issa, M.I. Sayyed, M.H.M. Zaid, K.A. Matori, A Comprehensive Study on Gamma Rays and Fast Neutron Sensing Properties of GAGOC and CMO Scintillators for Shielding Radiation Applications, J. Spec. (2017) 1 – 9.

[6] M.S. Al-Buriahi, B.T. Tonguc, Mass attenuation coefficients, effective atomic numbers and electron densities of some contrast agents for computed tomography, Radiat. Phys. Chem. 177 (2020) 108507.

[7] A.G.M. Santos, R.S.F. Dam, W.L. Salgado, R. Schirru, C.M. Salgado, Determination of mass attenuation coefficient of polylactic acid using gamma densitometry in 50 – 1000 keV energy range, Radiat. Phys. Chem. 177 (2020) 109097.

[8] A.W. El-Sayed, A.F. Michael, A.B. Mohamed, Gamma–ray mass attenuation coefficient and half value layer factor of some oxide glass shielding materials, Ann. Nucl. Ene. 96 (2016) 26 – 30.

[9] S. Jagtap, P. Chopade, S. Tadepalli, A. Bhalerao, S. Gosavi, A review on the progress of ZnSe as inorganic scintillator, Opto-Electron. Rev. 27 (2019) 90 – 103.

[10] A. Phunpueok, V. Thongpool, S. Jaiyen, W. Chewpraditkul, Photoelectric Fraction and Total Mass Attenuation Coefficient of Ce:YAG, Ce:GAGG and Ce:LuAG Single Crystals at 662 keV Gamma Radiation Energy, Mater. Today–Proc. 17 (2019) 1494 – 1499.

[11] M. Bettiol, E. Preziosi, C. Borrazzo, C. Polito, M.N. Cinti, R. Pellegrini, R. Pani, $LaBr_3$:Ce and NaI:Tl performance comparison for single photon emission detector, Nucl. Instrum. Meth. A. 912(21) (2018) 154 – 157.

[12] L. Caifeng, Q. Jianguo, X. Jun, Z. Tonghua, L. Xinxin, A. Li, M. Yunfeng, Z. Pu, S. Junjie, J. Li, W. Mei, H. Zijie, Particle discrimination and fast neutron response for a NaIL:Tl and a NaI:Tl scintillator detector, Nucl. Instrum. Meth. A. 978(21) (2020) 164372.

[13] S. Khan, H.J. Kim, Y.D. Kim, Scintillation characterization of thallium-doped lithium iodide crystals, Nucl. Instrum. Meth. A. 793(1) (2015) 31 – 34.

[14] C. Michail, I. Valais, I. Seferis, N. Kalyvas, G. Fountos, I. Kandarakis, Experimental measurement of a high resolution CMOS detectorcoupled to CsI scintillators under X-ray radiation, Radiat. Meas. 74 (2015) 39 – 46.

[15] A. Kumar, M.I. Sayyed, M. Dong, X. Xue, Effect of PbO on the shielding behavior of $ZnO–P_2O_5$ glass system using Monte Carlo simulation, J. Non–Crystalline Solids. 481 (2018) 604 – 607.

[16] S.A.M. Issa, M. Ahmad, H.O. Tekin, Y.B. Saddeek, M.I. Sayyed, Effect of Bi_2O_3 content on mechanical and nuclear radiation shielding properties of $Bi_2O_3–MoO_3–B_2O_3–SiO_2–Na_2O–Fe_2O_3$ glass system, Results. Phys. 13 (2019) 102165.

[17] M.G. Dong, O. Agar, H.O. Tekin, O. Kilicoglu, K.M. Kaky, M.I. Sayyed, A comparative study on gamma photon shielding features of various germanate glass systems, Compos. Part B. 165 (2019) 636 – 647.

[18] O. Kilicoglu, E.E. Altunsoy, O. Agar, M. Kamislioglu, M.I. Sayyed, H.O. Tekin, N. Tarhan, Synergistic effect of La_2O_3 on mass stopping power (MSP)/projected range (PR) and nuclear radiation shielding abilities of silicate glasses, Results. Phys. 14 (2019) 102424.

[19] O. Agar, E. Kavaz, E.E. Altunsoy, O. Kilicoglu, H.O. Tekin, M.I. Sayyed, T.T. Erguzel, N. Tarhan, Er_2O_3 effects on photon and neutron shielding properties of $TeO_2–Li_2O–ZnO–Nb_2O_5$ glass system, Results. Phys. 13 (2019) 102277.

[20] B. Oto, N. Yıldız, T. Korkut, E. Kavaz, Neutron shielding qualities and gamma ray buildup factors of concretes containing limonite ore, Nucl. Eng. Des. 293 (2015) 166 – 175.

[21] P. Lecoq, Development of new scintillators for medical applications, Nucl. Instrum. Methods Phys. Res. Section A. 809 (2016) 130 – 139.

[22] J. Glodo, Y. Wang, R. Shawgo, C. Brecher, R.H. Hawrami, J. Tower, K.S. Shah, New Developments in Scintillators for Security Applications, Physcs. Proc. 90 (2017) 285 – 290.